ISSN NO. 2320-5407

Journal homepage: http://www.journalijar.com

INTERNATIONAL JOURNAL OF ADVANCED RESEARCH

RESEARCH ARTICLE

Raman, photoluminescence and low temperature synchrotron X-ray powder diffraction studies of lanthanum orthovanadate

***M. Nasir Khan[1], Taj. Muhammad[2] and J. Bashir[1]**

1. Physics Division, Pinstech, P.O. Nilore, 45500, Islamabad.

2. Nilop, P. O. Nilore, 45600, Islamabad.

Manuscript Info

Manuscript History:

Received: 08 October 2013
Final Accepted: 27 October 2013
Published Online: November 2013

Corresponding Author

M. NASIR KHAN

Abstract

Pure monoclinic phase of $LaVO_4$ was successfully obtained through solid state reaction technique and has been characterized for low temperature phase transition studies by synchrotron X-ray diffraction. The room temperature Raman spectroscopic and photoluminescent measurements were also carried out to investigate the optical properties of this material. The synchrotron powder X-ray diffraction data refined by Rietveld refinement method revealed a stable monoclinic structure from 140K to room temperature with space group $P2_1/n$ (a non standard setting of $P2_1/c$ No 14). The lattice constants showed slight variation with increasing temperature. The lattice constants at room temperature; a = 7.0051(1) Å; b = 7.2414(2)Å; c = 6.6843(1) Å; β =104.86(1)°, V = 339.07(3) Å^3, Z = 4, D_x = 5.03 gm.cm^{-3} are in good agreement with the earlier single crystal and bulk polycrystalline X-ray diffraction results. The materials showed superior optical properties when compared with the earlier published data on bulk and nonmaterial of this system.

I. Introduction

Rare earth compounds are widely used in many practical applications because of their peculiar properties originating from unique electronic structure and numerous transition modes involving 3d and 4f shell of lanthanide [1-8] Lanthanide (Ln^{3+}) orthovanadate possessing chemical formula ABO_4 (where A is lanthanide and B = vanadate) are technologically important materials with immense applications as catalysis, efficient phosphors, low threshold laser host, solid-state protonic conductor and polarizer [9-11]. Lanthanum orthovanadate $LaVO_4$ has attracted much interest of the researchers for the last one decade both from a fundamental point of view and from the prospect of applications due to its surface catalytic properties. Being the binary oxide of vanadium it is effectively utilized as catalysts for vapour phase dehydrogenation of parafins [12, 13]. $La_xSr_{1-x}VO_3$ doped lanthanum vanadates have been extensively studied for their structural, magnetic and conductive properties [14-17], whereas vanadates containing V^{5+} are being studied for the selective oxidative dehydrogenation of propane, butane and ethylbenzene [18-20]. Reduced and oxidized lanthanum vanadates doped with strontium have been studied by Trikalitis *et al* [21] for their surface catalytic properties.

Lanthanum orthovanadates crystallizes in two polymorphs; a metastable tetragonal phase (t) and monoclinic phase (m). It is now well established that due to much larger ionic radii of La^{3+} ion in all lanthanide group, monazite (m-$LaVO_4$) are thermodynamically more stable than the metastable tetragonal (t-$LaVO_4$) due to its higher oxygen coordination number 9 compared with 8 of the t-orthovanadate, a much resolved problem with the structure of this materials over the last few years [22-24]. Previously it has been reported that m-$LaVO_4$ is neither a suitable host for luminescent activators nor a promising catalyst [25, 26] while t-$LaVO_4$ is anticipated to possess some excellent properties [27]. Selective synthesis of m- and t-$LaVO_4$ nanocrystals was performed recently to address issue like phase change processes, structure-dependent properties, and their potential applications but no appreciable improvement in either of the properties have been achieved in nanocrystalline t-$LaVO_4$ structure [28-30]. Lanthanum orthovanadate is considered to play a crucial role in optics, magnetic and catalytic field in future [31-

34]. The lanthanide compounds reveal interesting structural and magnetic transformations at low temperatures and exceptionally few undergo John-Teller distortions [35, 36]. The 3d electron configuration of La^{3+} ($3d^{10}$) is reported to exhibit antiferromagnetism at certain temperatures range below room temperature down to 140K. Therefore the interplay of orbital, spin and vibrational motions of V^{5+} and La^{3+} ions may lead to a sequence of phase transitions involving changes in the structural magnetic and optical properties of this compound [37]. In order to reveal such phenomenon in monazite $LaVO_4$, low temperature synchrotron X-ray diffraction measurements were carried out to study structural phase transition in this material along with Raman and photoluminescence studies at room temperature to characterize the structure-property relationship and its potential applications.

II. EXPERIMENT

Polycrystalline sample of $LaVO_4$ was prepared through solid-state reaction technique. The mixture of appropriate amounts of 99.99% La_2O_3 and V_2O_5 was first heated at 1000 ^oC for 17 hours followed by two 13 hours heating at 1200 $^\circ C$ with intermediate grinding after each step. Once the single-phase material was obtained, it was annealed at 1250 ^oC for 17 hours to improve the crystallinity. Synchrotron X-ray powder diffraction measurements were performed on XRD1 beam line at ELETTRA, Trieste, Italy, which is equipped with a double- Si(111) crystal monochromator in non-dispersive configuration followed by a toroidal focusing mirror with a horizontal acceptance of 2.8 mrad. The sample was contained in quartz capillary (0.3 mm dia). MARS345 imaging plate was used to record the diffraction pattern with sample to detector distance of 200mm. The wavelength was 0.70Å. The series of two dimensional powder diffraction data were converted into one dimensional powder patterns (2θ versus intensity) by using Fit2D [38]. Wavelength and distance calibration were carried out from LaB_6. Oxford Cryosystems (series 700) was employed to measure the low temperature diffraction data down to 140K. To investigate different phonon modes and phases in the sample, vibrational spectroscopy was carried out using Raman spectroscopy system model MST-4000A Dongwo Optron Ltd. To focus the sample, it was illuminated by ordinary flash light through objective lens (100X/0.70, f = 200). After focusing in image mode, the sample was shined by intense He-Cd laser source with wavelength 442 nm/80.0 mW and beam diameter 2.00 mm. The signals were collected and detected in scan mode by the same objective lens and air cooled at the rate -50^oC CCD detector. The Rayleigh peak at 442nm was eliminated by using 442nm cut-off filter. The spectrum was taken in the range from 200 cm^{-1} to 1000 cm^{-1} using DM320 monochromator and ANDOR DV 401A-BV CCD software. The accumulate acquisition mode was used to reduce noise and thermal fluctuation greatly with improved S/N ratio. For photoluminescence measurements same setup was used except that the sample was shined with same laser source with wavelength 325 nm.

III. DATA ANALYSIS

The Synchrotron X-ray powder diffraction data were analyzed by Rietveld profile analysis technique using programme Rietica [39]. Peak shapes were described by Pseudo-Voigt function and background was fitted by a fifth order polynomial. Refined parameters included unit cell parameters, position and individual thermal parameters as well as the usual profile parameters describing the pseudo-Voigt peaks shape function. For diminishing the severe peak overlap, intensities within five times of the full width at half maximum (FWHM) were considered to contribute to a particular reflection.

As a starting point of the refinement, structural parameters were taken from previous published papers [24, 40] in space group $P2_1/n$ that is a non-standard setting of $P2_1/c$ (No.14). A total of 37 parameters were refined which included four background parameters, the instrument zero point, six profile parameters, cell dimensions, scale factor, fractional atomic coordinates and thermal parameters of each atom in their respective valence state. The preferred orientation (001) correction due to presence of platy crystallites in the sample was carried out according to W. Pitschke et.al and Dollase [41-42].[41-42] The Raman shift and damping factors for different modes of vibrations was extracted from the observed spectra by describing the different modes as damped harmonic oscillator (DHO) and was fitted by DHO equation below;

$$y = \frac{2A_1}{\Pi}\left(\frac{\omega_{10}}{4(x-x_c)+\omega_1^2}\right) + \frac{A_2\tau}{1+(x-x_c)^2\tau^2} + \sum_{j>2}\frac{A_j\omega_{j-2}g_{j-2}}{\left[\omega_{j-2}^2-(x-x_c)^2\right]^2+(x-x_c)^2 g_{j-2}^2} + B_g$$

The first term in the above equation is the Lorenztian function for Rayleigh peak, the second term represents the Debye related functions. B_g is the background and the third term is damped harmonic oscillator functions

considering non -coupled modes. Rests of the notations in the equation are related to amplitude, peak position, full width and half maxima of peaks etc.

IV. RESULTS AND DISCUSSION

The refined synchrotron X-ray diffraction patterns at 140 and 300 K are shown in Fig. 1. In the same figure, satisfactory matching of experimental with calculated values of the synchrotron X-ray diffraction data can be appreciated from the curve shown at the bottom of figure that corresponds to the difference between the observed and calculated diffraction patterns. The refined unit cell parameters and unit cell volume along with mean bond distances are listed in Tables 1& 2.

The refinement results revealed a stable flexible MXO_4 structure type containing approximately tetrahedral XO_4 units and M cations with irregular nine-fold coordination with anion atoms down to 140 K and are in agreement to the earlier findings [24, 40, 41, 43]. Fig. 2 shows the lattice constants variation with temperature showing a linear tendency with temperature without any appreciable change in the unit cell volume. The structure at 300 K with view in (001) direction is shown in Fig. 3. The bond distances has been labelled at respective VO_4 tetrahedral (numeric in parenthesis) and LaO_9 polyhedral (numeric underlined) with the respective oxygen atoms. Each vanadium atom is at the centre of distorted tetrahedron of oxygen atoms with four V-O distances ranging from 1.639(1) Å to 1.747(1) Å, while La exhibits an irregular coordination by nine oxygen atoms in the range of 2.455(1)Å to 2.906(1) Å. In the crystal structure of $LaVO_4$ shown in Fig. 3 the VO_4 tetrahedra are isolated from each other, showing limited strong bonding between La and VO_4 tetrahedra. Each lanthanum atom is coordinated with two vanadium atoms at a distances of 3.371(1) Å and 3.824(2) Å. Further each La cation links with one of the O atom of the two VO_4 tetrahedra in the (001) direction showing strong bonding in this direction. The nature of bonding in both LaO_9 polyhedra and VO_4 tetrahedra are partially covalent due to the Pauling electronegativities of the La, V and O atoms. The four oxygen atoms around each vanadium atom in tetrahedral arrangement possess different bond lengths and tetrahedral are considerably distorted showing the O-V-O angles of 102.30(2)° to 115.70(2)° as can be revealed by data in Table 2.

Fig. 4 shows the Raman spectra of the sample at room temperature. The positions assigned to intense Raman bands are 849 $cm^{-1}$and 365 cm^{-1} having shoulders at 792 cm^{-1} and 339 cm^{-1} respectively. Besides this three weaker bands are visible at 243, 206 and 157 cm^{-1}. The Raman spectra of crystalline $LaVO_4$ reflect the VO_4 type tetrahedral structure that consist four different V–O bonds in agreement to the synchrotron x-ray diffraction data results (Fig. 3) . According to the interpretation of Hardcastle et al. [44], the most intense Raman band at about 849 cm^{-1} can be assigned to the symmetric V–O stretching mode (A_g symmetry), while the weak shoulder around 792 cm^{-1} is assigned to antisymmetric V–O stretching mode (B_g symmetry), the symmetric (A_g) and antisymmetric (B_g) bending modes are at 365 and about 3397 cm^{-1}, respectively, and external modes (rotation/translation) occur at 243, 206 and 157 cm^{-1}. The Raman bands and their assignments have been reported in Table 3. The position for the assigned Raman bands shown in this study has a similarity to the bismuth vanadate samples with similar monoclinic structure also containing VO_4 tetrahedron [45].

Table 1. Comparison of unit cell parameters with literature

	Bashir et al [24]	Baran & Aymonino [43]	Present Work
Space Group	$P2_1/n$ (14)	$P2_1/m$ (11)	$P2_1/n$ (14)
a(Å)	7.0434(1)	7.07	7.0051(1)
b(Å)	7.2801(1)	7.29	7.2414(2)
c(Å)	6.7224(1)	6.77	6.6843(1)
β°	104.865(1)	105	104.87(1)
***Density* (*gm cm*$^{-3}$)**	5.07	5.0	5.03(2)

Table 2. Bond distances (Å) for $LaVO_4$ at room temperature

Lanthanum polyhedron		**Vanadium tetrahedron**	
La – O3	2.488(1)	V – O1	1.747(1)
La – O4	2.479(1)	V – O2	1.644(1)
La - O1	2.476(1)	V – O4	1.715(1)
La – O4	2.556(1)	V – O3	1.639(1)
La – O1	2.455(1)	**Average**	1.6863(1)
La – O2	2.588(1)	∠O2-V-O4	115.70°
La – O2	2.615(1)	∠O3-V-O4	102.30°
La - O2	2.906(1)		
La – O3	2.646(1)	La - V	3.371(1)
Average	2.5788(1)	La - V	3.824(2)

Table 3: Raman and PL data of $LaVO_4$ at room temperature

Peaks	Position	FWHM	Assigment	Symmetry
	Raman Data			
1.	157	11.89	La-O Rot/trans	External
2.	206	46.33	La-O Rot/trans	External
3	243	14.94	La-O Rot/trans	External
4.	339	48.12	Antisymmetric V-O bending mode	B_g symmetry
5.	365	78.41	Symmetric V-O bending mode	A_g symmetry
6.	792	34.15	Antisymmetric V–O stretching mode	B_g smmetry
7.	849	30.88	Symmetric V–O stretching mode	A_g symmetry
Photoluminescence Data				
1.	338nm (3.67eV)		intravanadate transition	
2.	365nm (3.39eV)		VO_4^{3-} group emissions	
3.	454nm (2.74eV)		VO_4^{3-} group emissions	

Rot. (Rotational) & Trans. (translational)

Fig. 1: Refined Synchrotron X-ray diffraction patterns for $LaVO_4$ (a) 140 K (b) 300 K, observed (+), and calculated (-). Bottom curve shows appreciable matching between observed and calculated pattern. The reflections positions are also marked.

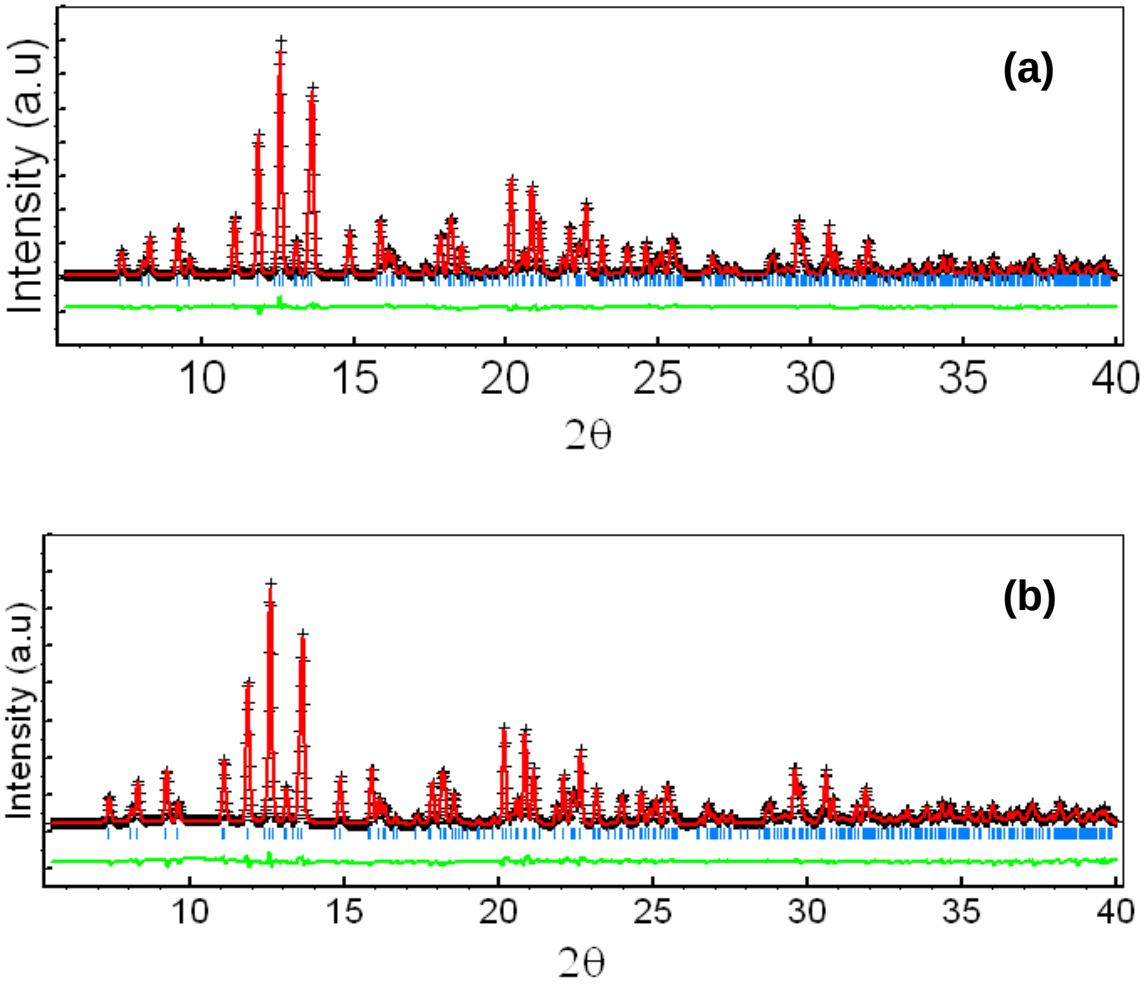

Fig. 2: Variation of the lattice constants with temperature

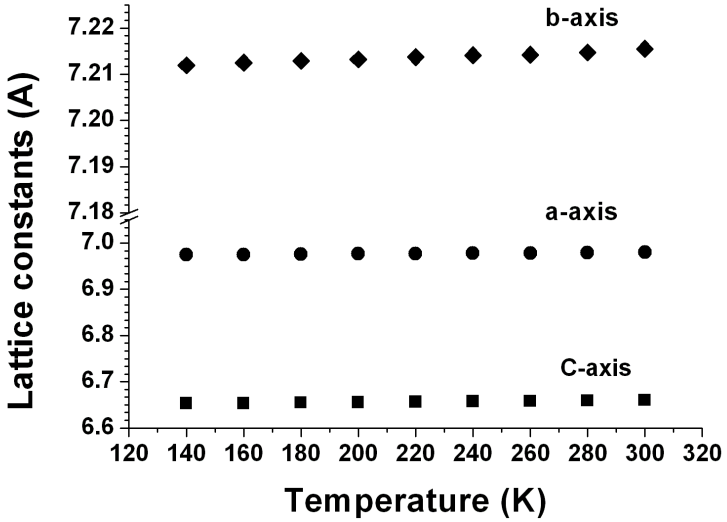

Fig. 3: Crystal structure of $LaVO_4$, at 300 K with view in (001) direction showing that each vanadium atom is at the centre of distorted tetrahedron of oxygen atoms.

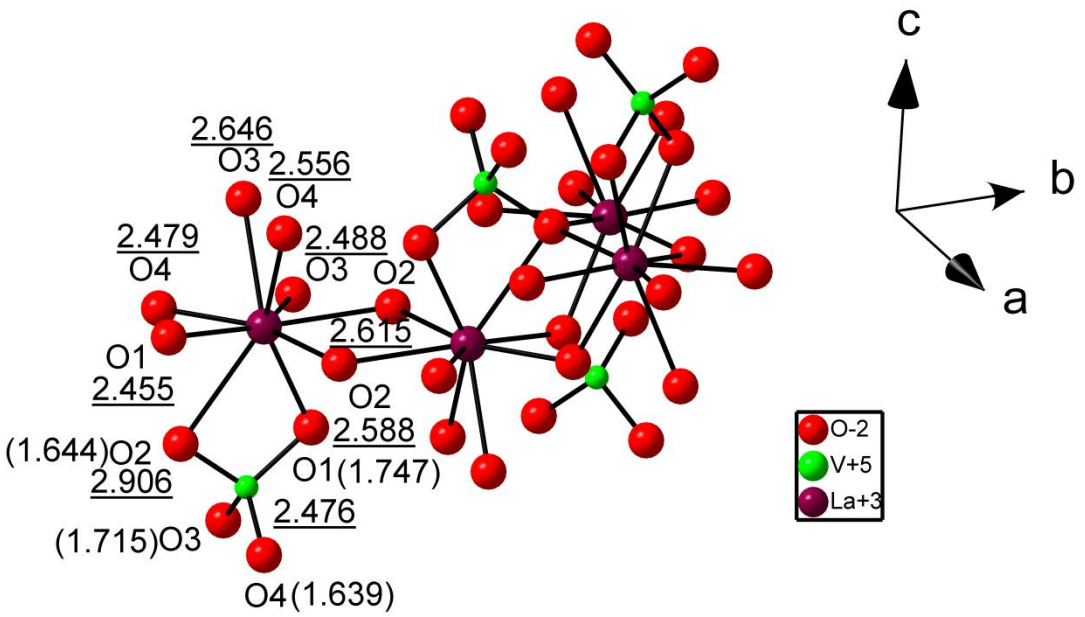

Fig. 4: Room temperature Raman Spectrum of bulk m-$LaVO_4$

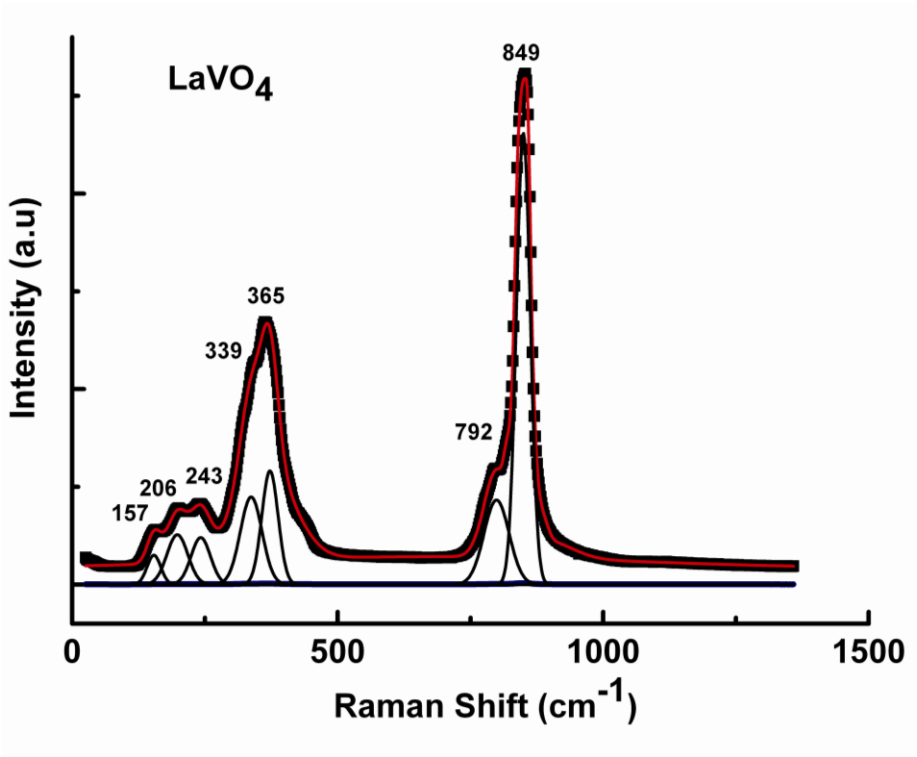

Fig. 5: Room temperature photoluminescence spectrum of bulk m-$LaVO_4$

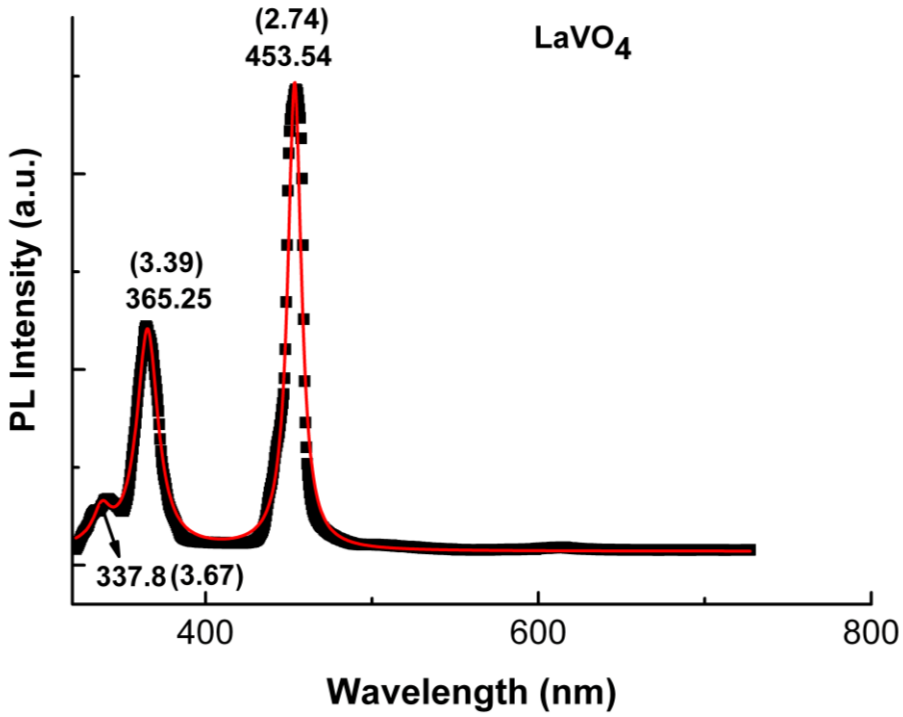

The position of the more intense Raman band at 849 cm^{-1} at higher wave numbers reveals that the average short-range symmetry of the VO_4 tetrahedra is not regular [43], and is agreement with the synchrotron X-ray diffraction data where the VO_4 tetrahedron are well isolated and bond lengths varies in all the three axes showing highly distorted structure (Fig 3). On the contrary, lower values of FWHM of the band for the sample prepared by solid-state reaction at higher temperature reveal better crystallinity of the sample. These Raman results are not in contradiction, because the Raman band positions are very sensitive to the short range order, whereas the Raman widths are more sensitive to the degree of crystallinity, defects and disorders, particle size and/or aggregation of particles. Therefore, the Raman results imply that sample prepared at high temperature by solid state reaction consist of less symmetric but distorted VO_4 tetrahedra but possess better crystallinity.

Fluorescence spectroscopy is another valuable tool providing information about the intermolecular interactions of different atoms in crystals and monolayers [46]. Room-temperature photoluminescence (PL) spectra of the high temperature synthesized $LaVO_4$ monoclinic polycrystalline sample was measured with excitation wavelength of 325 nm using He-Cd laser and are shown in Fig. 5. Two well defined sharp and prominent emissions, peaking at 365nm (3.39 eV) and 454 nm (2.74 eV), were observed along with a shoulder at nearly 338nm (3.67eV) in agreement to the PL emission spectra of monoclinic $LaVO_4$ nanoparticles. PL peaks shape and intensities are for better in our sample when compared to the data of nanoparticles of the same material with similar monoclinic structure [47-48]. The band at 338 nm (3.67 eV) identified as the intravanadate transition, $V^{5+}O_4^{8-} \rightarrow V^{4+}O_4^{7-}$ providing information about the band gap of the material and is the symmetry forbidden $1A_1 \rightarrow 1T_1$ ($t_1 \rightarrow e$) defining the band gap energy as the energy between the top of the valence band and bottom of the conduction and is in agreement to the earlier finding of A. H. Krumpel et. al [49]. The peaks at 365nm and 454nm are the characteristic VO_4^{3-} group emissions due to the self absorption in this material.

From the PL and Raman spectroscopy results we elucidate that optical properties shown in our work by monazite $LaVO_4$ are comparable to that of the tetragonal zircon type $LaVO_4$ [47-48] as the structure of monazite is similar to that of zircon in several ways. In monazite, isolated VO_4 tetrahedra share corners and edges with LaO_9 polyhedra, which superficially resemble LaO_8 dodecahedra in zircon. The La polyhedra in monazite share edges with each other to form chains parallel to the a-axis (Fig. 3) that resemble analogous LaO_8 dodecahedral chains in zircon. The La atom in monazite is coordinated by nine O atoms as described by synchrotron x-ray diffraction data. The four axial O atoms (two each forming the shared edge with two adjacent VO_4 tetrahedra) and five equatorial O atoms. The equatorial O atoms are each part of five neighboring VO_4 tetrahedra that share their corners with the *La*

polyhedron. Thus the La polyhedron in monazite shares corners and edges with seven neighbouring VO_4 tetrahedra, whereas the LaO_8 polyhedron in zircon shares polyhedral elements with six VO_4 tetrahedra. The four axial O atoms define a distorted LaO_4 tetrahedron elongated along [001], analogous to the LaO_4 tetrahedron in zircon. The edge-sharing V and La polyhedral chains along [001] in monazite closely resemble the [001] polyhedral chains in zircon, although the chains in monazite are twisted compared to those in zircon. The zircon structure can be visualized as two interpenetrating arrays of alternating, corner-sharing VO_4 and LaO_4 tetrahedra. Owing to nine O atoms being coordinated to La in monazite, the LaO_9 polyhedron cannot be adequately described as two interpenetrating tetrahedra. The ninth La-O bond in monazite can be seen as arising from a twisting of polyhedra in monazite relative to analogous polyhedra in zircon, which results in an additional bond between VO_4 group and the LaO_9 polyhedron. The arrays of VO_4 and LaO_4 tetrahedra, which are independent in the zircon structure, are no longer independent in monazite, due to the ninth La-O bond. Thus, monazite has greater overall structural connectivity than does zircon. The structure of monazite is more densely packed and space filling than zircon and it lacks the interstitial voids and channels present in the zircon structure as can be seen from the Raman and photoluminescence data of this high temperature synthesized monazite $LaVO_4$ sample when compared to data of t-$LaVO_4$. The interstitial voids and channels usually present is nanocrystalline t-$LaVO_4$ may be a possible reason for a slight red shift in the PL data for the t-$LaVO_4$ [47-48].

V. CONCLUSION

The present study concludes that $LaVO_4$ is monoclinic with space group $P2_1/n$ with tetra-molecular cell is stable down to low temperature of 140K. The lattice constants determined by Rietveld refinement method did not show any appreciable change showing nearly a constant volume down to 140K temperature. No phase transition was found in the measured temperature range. The average V-O distances slightly changes with temperature mainly due to the arrangement of oxygen atom around V and La ion in this structure. The monazite $LaVO_4$ has close resemblance to t–$LaVO_4$ in the corner and edge sharing mechanism of isolated VO_4 and La-O polyhedron and can be equally regarded as potential materials for optical applications as revealed from the Raman and photoluminescent studies on this material.

REFERENCES

[1] S. Ishihara, Phys. Rev. Lett. 94 (2005) 156408.
[2] S. Ishihara and T. Hatakeyama, J. Mag. Mag. Mater. 272 (2004).412
[3] C. Ulrich, G. Khaliullin, and C. Mirker, Phys. Rev. Lett. 91(2003) 257202.
[4] Z. Fang, N. Nagaosa and K. Terakura, Phys. Rev. B 67(2003)035101.
[5] S. Miyasakal, Y. Okimoto and Y. Tolura, J. Phys. Soc. Jpn.71 (2002) 2086.
[6] B. Bleaney, J. Z. Pfeffer and M. R. Wells, J. Phys.: Condens. Matter 9 (1997) 7469
[7] Y. Motome, H. Seo and Z. Fang, Phys. Rev. Lett. 90 (2003)146602.
[8] J. Q. Yan, J. S. Zhou and J. B. Goodenough, Phys. Rev. Lett. 93 (2004) 235901
[9] Z.M.Fang, Q. Hong, Z.H. Zhou, S.J. Dai, W.Z. Weng and H. L. Wan, Catal Lett., 61(1999)39.
[10] B.C. Chakoumakos, M. M. Abraham and L.A. Boatner, J. Sol. Stat. Chem. 109 (1994)197
[11] Y.Oka, T. Yao and N. Yamamoto, J. Sol. Stat. Chem.152 (1994) 486
[12] A. T.Guttmann, J. F. Brazdil and P. K. Grasselli, US Patent, 4-816-243, 1989
[13] M. R. Balasubramanian, J. Indian Chem. Soc. 64 (1978) 453
[14] B. Reuter and M. Vollnik, Naturwissenschaften, 50 (1963) 569
[15] R. G. Egdell, M. R. Harrison, M. D. Hill, L. Porte and G. Wall, J. Phys. C17 (1984) 2899
[16] P. Dougier, A. Casalot, J. Sol. Stat. Chem.15 (1970) 346
[17] P. Dougier, P. Hagenmuller, J. Sol. Stat. Chem. 15 (1975) 158
[18] M.C. Kung, H. H. Kung, J. Catal. 134 (1992) 668
[19] X. Gao, P. Ruitz, Q. Xin, B. Delmon, J. Catal. 148 (1994) 56
[20] W.S. Chang, Y.S. Chen, B. L. Yang, Appl. Catal. A: General, 124 (1995)221
[21] P. N. Trikalitis, T. V. Bakas, A. C. Moukarika, A. T. Sdoukos, T. Angelidis, P. J. Pomonis, Appl. Catal. A167 (1998) 295
[22] C. J. Jia, L. D. Sun, L. P. You, X. C. Jiang, F. Luo, Y. C. Pang, C. H. Yan, J. Phys. Chem. B 109 (2005) 3284
[23] J. Isasi, M. L. Veiga, F. Fernandez, C. Pico, J. Mater. Sci. 31(1996) 4689
[24] J. Bashir, M. Nasir Khan, Mater. Lett. 60 (2006) 470
[25] F.C. Palilla, A. K. Levine, M. J. Rinkevics, J Electrochem. Soc. 112 (1965) 776
[26] U. Rambabu, D. P. Amalnerkar, B. B. Kale, S. Buddhudu, Mater. Res. Bull. 35 (2000) 929

[27] C. J. Jia, L. D. Sun, F. Luo, X. C. Jiang, L. H. Wei, C. H. Yan, Appl. Phys. Lett. 84 (2004) 5305
[28] R. Yan, X. Sun, X. Wang, Q. Peng, Y. D. Li, Chem. Eur. J., 11 (2005) 2183
[29] X. Y. Chen, L. Yang, R. E. Cook, S. Skanthakumar, D. Shi, G. K. Liu, Nanotechnology. 14 (2003)670
[30] W. Fan, X. Song, Y. Bu, S. Sun, X. Zhao, J. Phys.Chem. B110 (2006) 23247
[31] Z. M. Fang, Q. Hong, Z. H. Zhou, S. J. Dai, W. Z. Weng, H. L. Wan, Catal. Lett. 61 (1999)39
[32] R. A. Fields, M. Birnbaum, C. L. Fincher, Appl. Phys. Lett. 51 (1987) 1885
[33] M. R. Balasubramanian, J. Ind. Chem. Soc. 64 (1987) 453
[34] V. Buissette, A. Huignard, T. Gacoin, J. P. Boilot, P. Aschehoug, B. Viana., Surf. Sci., 532 – 535 (2003) 444
[35] G. A Ghering, K. A. Ghering., J. Mater. Sci. Lett. 2 (1975) 371
[36] S. H. Smith, B.M. Wanklyn, J. Cryst. Growth, 21 (1974) 23
[37] N. Wang, Q.Zhang, W. Chen, Cryst. Res. Technol. 42 (2007)138
[38] A. P. Hammersley, S. O. Svensson, M. Hanfland, A. N. Fitch, D. Hausermann, High Press. Res. 14 (1996) 235
[39] C.J. Howard, B. A. Hunter (1998); " A computer programme for Rietveld analysis of X-ray and Neutron Powder Diffraction Patterns" Lucas Heights Research Laboratories., NSW, Australia pp1-27
[40] C.E. Rice, W Robinson, Acta Cryst. B3 (1976) 2232
[41] W. Pitschke, H. Hermann, and N. Mattern, Powder Diffraction, 8 (1993) 74
[42] W.A. Dollase, J. Appl. Cryst. 19 (1986) 267
[43] E. J. Baran, P. J. Z Aymonino,. Anorg. Allgem. Chem. 383(1971)220 and Powder Diffraction file JCPDS 25-427
[44] F.D. Hardcastle, I.E. Wachs, H. Eckert, D.A. Jefferson, J. Sol. Stat.Chem.90 (1991) 194
[45] M. Gotic, S. Music, M. Ivandaa, M. Soufek, S. Popovic, J. Mol. Struc. 744–747 (2005) 535
[46] Y. Hu, J.F. Chen, W.M. Chen, X.H. Lin, X.L. Li, Adv. Mater. 15 (2003)726
[47] H.W. Liao, Y.F. Wang, X.M. Liu, Y.D. Li, Y.T. Qian, Chem.Mater. 12 (2000)2819
[48] W. Fan, W. Zhao, L. You, X. Songa, W. Zhanga, H. Yu, S. Sun, J. Sol. Stat. Chem. 177 (2004) 4399
[49] A. H. Krumpel, E. Van der Kolk, E. Cavalli, P. Boutinaud, M. Bettinelli, P. Dorenbos, J. Phys. C 21(2009)115503